# Mitochondrial metabolism sets the maximal limit of fuel-stimulated insulin secretion in a model pancreatic beta cell: a survey of four fuel secretagogues

Antinozzi, Peter; Ishihara, Hisamitsu; Newgard, Christopher B; Wollheim, Claes

**How to cite**

ANTINOZZI, Peter et al. Mitochondrial metabolism sets the maximal limit of fuel-stimulated insulin secretion in a model pancreatic beta cell: a survey of four fuel secretagogues. In: The Journal of biological chemistry, 2002, vol. 277, n° 14, p. 11746–11755. doi: 10.1074/jbc.M108462200

This publication URL: https://archive-ouverte.unige.ch/unige:34526
Publication DOI: 10.1074/jbc.M108462200

THE JOURNAL OF BIOLOGICAL CHEMISTRY
Vol. 277, No. 14, Issue of April 5, pp. 11746–11755, 2002

*Printed in U.S.A.*

# Mitochondrial Metabolism Sets the Maximal Limit of Fuel-stimulated Insulin Secretion in a Model Pancreatic Beta Cell

A SURVEY OF FOUR FUEL SECRETAGOGUES*

Received for publication, September 4, 2001, and in revised form, December 27, 2001
Published, JBC Papers in Press, January 30, 2002, DOI 10.1074/jbc.M108462200

**Peter A. Antinozzi‡§, Hisamitsu Ishihara‡, Christopher B. Newgard¶, and Claes B. Wollheim‡**

*From the ‡Division of Clinical Biochemistry and Experimental Diabetology, Department of Internal Medicine, University Medical Center, CH-1211 Geneva 4, Switzerland and from the ¶Touchstone Center for Diabetes Research, Departments of Biochemistry and Internal Medicine, University of Texas Southwestern Medical Center, Dallas, Texas 75390*

**The precise metabolic steps that couple glucose catabolism to insulin secretion in the pancreatic beta cell are incompletely understood. ATP generated from glycolytic metabolism in the cytosol, from mitochondrial metabolism, and/or from the hydrogen shuttles operating between cytosolic and mitochondrial compartments has been implicated as an important coupling factor. To identify the importance of each of these metabolic pathways, we have compared the fates of four fuel secretagogues (glucose, pyruvate, dihydroxyacetone, and glycerol) in the INS1-E beta cell line. Two of these fuels, dihydroxyacetone and glycerol, are normally ineffective as secretagogues but are enabled by adenovirus-mediated expression of glycerol kinase. Comparison of these two particular fuels allows the effect of redox state on insulin secretion to be evaluated since the phosphorylated products dihydroxyacetone phosphate and glycerol phosphate lie on opposite sides of the NADH-consuming glycerophosphate dehydrogenase reaction. Based upon measurements of glycolytic metabolites, mitochondrial oxidation, mitochondrial matrix calcium, and mitochondrial membrane potential, we find that insulin secretion most tightly correlates with mitochondrial metabolism for each of the four fuels. In the case of glucose stimulation, the high control strength of glucose phosphorylation sets the pace of glucose metabolism and thus the rate of insulin secretion. However, bypassing this reaction with pyruvate, dihydroxyacetone, or glycerol uncovers constraints imposed by mitochondrial metabolism, each of which attains a similar maximal limit of insulin secretion. More specifically, we found that the hyperpolarization of the mitochondrial membrane, related to the proton export from the mitochondrial matrix, correlates well with insulin secretion. Based on these findings, we propose that fuel-stimulated secretion is in fact limited by the inherent thermodynamic constraints of proton gradient formation.**

The pancreatic islet beta cell secretes insulin in response to several metabolic fuels, and this occurs via the metabolism of the stimulatory agents rather than their interaction with a receptor (summarized by Newgard and McGarry, see Ref. 1). Fuel secretagogues such as glucose are metabolized to generate ATP. The increased ATP:ADP ratio inhibits ATP-sensitive $K^+$ ($K^+_{ATP}$) channels, which in turn causes depolarization of the plasma membrane, $Ca^{2+}$ entry through voltage-gated L-type $Ca^{2+}$ channels, and activation of exocytosis of insulin-containing secretory granules. The requirement for fuel metabolism and nucleotide generation is also observed in the presence of depolarizing concentrations of $K^+$ combined with diazoxide, which prevents $K^+_{ATP}$ channel closure, and this has been termed the $K^+_{ATP}$ channel-independent pathway of glucose-stimulated insulin secretion (GSIS)[1] (2–4). Whereas the effects of $K^+_{ATP}$ channel inhibition and calcium entry on insulin release are widely acknowledged, the source of ATP that regulates the ion channels and the potential involvement of other factors remain as open questions.

ATP is generated by both cytosolic and mitochondrial reactions. Cytosolic ATP production comes from two reactions in the distal portion of glycolysis, 3-phosphoglycerate kinase and pyruvate kinase. Mitochondrial ATP is derived in part from hydrogen shuttles, primarily the malate-aspartate (5–7) and glycerophosphate shuttles, (8–10) which are very active in islet beta cells. Finally, a major portion of ATP production comes from mitochondrial oxidation of glucose-derived pyruvate. There is evidence to support an important role of each of these discrete sources of ATP in the regulation of insulin secretion. Evidence for a role of glycolysis-derived ATP comes from studies in which inhibitors of glycolytic but not mitochondrial ATP-producing reactions inhibited GSIS (11). Evidence for an important role of hydrogen shuttles comes from studies showing near complete impairment of GSIS in islets from mice lacking mitochondrial glycerol phosphate dehydrogenase and incubated with aminooxyacetate to inhibit their malate-aspartate shuttle activity (12, 13). Finally, GSIS is impaired by inhibitors of oxidative phosphorylation (14) and mitochondrial uncouplers (15) and in cells with impaired mitochondrial function (16–19), supporting a role of ATP derived from fuel oxidation.

Stimulation of islets with fuels other than glucose suggests that important coupling factors are generated via cytosolic metabolism. The so-called "pyruvate paradox" is one such example because the mitochondrial fuel pyruvate is readily oxidized in islet preparations but does not elicit insulin secretion

* This study was supported by Grant 32-49755.96 from the Swiss National Science Foundation (to C. B. W.) and by a European Union Network Grant (through the Swiss Federal Office for Education and Science). The costs of publication of this article were defrayed in part by the payment of page charges. This article must therefore be hereby marked "*advertisement*" in accordance with 18 U.S.C. Section 1734 solely to indicate this fact.

§ To whom correspondence should be addressed. Tel.: 41-22-702-5554; Fax: 41-22-702-5543; E-mail: Peter.Antinozzi@clocs.com.

[1] The abbreviations used are: GSIS, glucose stimulated insulin secretion; Ad-GlpK, adenoviral-mediated glycerol kinase; Ad-CAG-mAeq, adenoviral-mediated mitochondrial targeted aequorin; DHA, dihydroxyacetone; DHAP, dihydroxyacetone phosphate; GAP glyceraldehyde phosphate; FBP, fructose 1,6-bisphosphate; PMA, phorbol 12-myristate 13-acetate; KRBH, Krebs-Ringer bicarbonate buffer; FCCP, carbonyl cyanide *p*-trifluoromethoxyphenylhydrazone.

(20, 21). In contrast, glyceraldehyde, which functions both as a cytosolic and mitochondrial fuel, is a potent secretagogue (22–24). In another study, the glycolytic intermediate glyceraldehyde phosphate (GAP) stimulated insulin release from pancreatic islets, and this effect was not impaired by mitochondrial inhibitors (15). However, glyceraldehyde can be converted to the non-metabolizable intermediate glycerate-1-phosphate while still generating NADH (25) and can cause acidification of the cytosol (26–28), making it difficult to fully interpret experiments with this secretagogue. Acidification has also been observed in studies with another widely used metabolite analog, methyl pyruvate (29, 30). Since acidification alone can stimulate ATP generation in isolated mitochondria, the use of such compounds to dissect the role of cytosolic and mitochondrial signal generation could be misleading.

To clarify the roles of cytosolic and mitochondrial metabolism of carbohydrate fuels in the regulation of insulin secretion, we developed a novel strategy to provide metabolic input at the point of triose metabolism (31). Due to low glycerol phosphorylating activity, pancreatic beta cells do not metabolize glycerol efficiently enough to elicit insulin secretion. However, with adenovirus-mediated expression of glycerol kinase, glycerol is efficiently metabolized, which allows the stimulation of insulin secretion (31) and proinsulin biosynthesis from a glycerol challenge (32). The advantage of this strategy is that the nonspecific effects of glycerol (*i.e.* side reactions, pH changes) are controlled by the inclusion of cells not engineered for glycerol kinase expression. Furthermore, as shown in the current study, glycerol kinase expression activates the conversion of dihydroxyacetone (DHA) to dihyroxyacetone phosphate (DHAP), thereby allowing DHA to become an insulin secretagogue. In the current study, we have measured the metabolic fates of four distinct carbohydrate fuels, glucose, pyruvate, glycerol, and DHA, in cells enabled for triose-stimulated insulin secretion by glycerol kinase expression. Neither large increases of glycolytic intermediates nor marked changes in the redox state influenced insulin secretion. Stimulation of secretion by these fuels most closely correlated to changes in the mitochondrial membrane potential, suggesting that the generation of the mitochondrial proton gradient, ATP, and other mitochondrially derived metabolites are essential signals for insulin secretion.

## MATERIALS AND METHODS

*Insulin Secretion and Metabolite Measurements*—INS1-E cells were cultured as described by Asfari *et al.* (33) and seeded at a density of $1.5 \times 10^6$ cells/well in a 6-well tissue culture plate (Falcon). One day prior to the experiment, the cells were transduced with Ad-GlpK virus (see Ref. 31 for details) and cultured in RPMI 1640 containing 5 mM glucose. Cells were washed 3 times with modified Krebs-Ringer bicarbonate buffer (KRBH) containing (in mM): 135 NaCl, 3.6 KCl, 10 HEPES (pH 7.4), 5 $NaHCO_3$, 0.5 $NaH_2PO_4$, 0.5 MgCl, and 1.5 $CaCl_2$ and preincubated for 30 min in KRBH with 2.5 mM glucose. Cells were washed an additional two times and incubated with KRBH supplemented with the appropriate secretagogue. After 15 min of incubation, medium was collected for insulin radioimmunoassay, and cells were quickly frozen in liquid nitrogen with the addition of 0.6 M perchloric acid. Extracts were collected on ice, sonicated, and centrifuged. The supernatant was neutralized with $K_2CO_3$, and DHAP, GAP, FBP, pyruvate, lactate, and glycerol phosphate were measured by the methods compiled by Bergenmeyer (34).

*Substrate Oxidation*—Oxidation assays were performed essentially as described by Antinozzi *et al.* (35). For each data point, $\sim 1 \times 10^6$ cells were resuspended in KRBH and dispensed into a center well placed within a scintillation vial. Radiolabeled substrate (~500,000 cpm [2-$^{14}$C]DHA or [2-$^{14}$C]glycerol) was diluted with unlabeled substrate and added to the cell suspension, and the vial was sealed with a rubber septum. After 1 h, 100 $\mu$l of 7% perchloric acid was injected into the center well, and 300 $\mu$l of benzethonium hydroxide was injected at the bottom of the vial. Following 5 h at room temperature, the center well was removed, liquid scintillation mixture was added to the vial, and the amount of [$^{14}CO_2$] generated was counted.

*Glycerol Kinase Activity*—Glycerol kinase activity was measured by an adaptation of the spectrophotometric method of Wieland and Suyter (36). The phosphorylation of glycerol was coupled to the reduction of NAD by the action of L-$\alpha$-glycerophosphate dehydrogenase. The reaction mixture contained 10 mM glycerol, 20 mM $MgCl_2$, 20 mM ATP, and 1.6 mM $NAD^+$ prepared in a hydrazine/glycine/EDTA (400 mM/1 M/5 mM) buffer at pH 9.5. Six units of L-$\alpha$-glycerophosphate dehydrogenase (Sigma) were added, and a baseline was established. The activity measurement was initiated with the addition of 50 $\mu$g of cell extract, and NADH absorbance was followed at 339 nm for 15 min. Activity was calculated from the slope of an absorbance *versus* time plot.

*Mitochondrial Membrane Potential*—INS1-E cells ($3 \times 10^6$) were centrifuged and resuspended in 2 ml of KRBH with 2.5 mM glucose and 10 $\mu$g/ml rhodamine-123 (Molecular Probes) for 10 min. Cells were centrifuged and resuspended in 2 ml of KRBH and transferred to a glass cuvette. After stabilization of the fluorescence signal for 15 min, secretagogues were sequentially added followed by a final addition of 1 $\mu$M FCCP. Changes in rhodamine-123 fluorescence were recorded every 3 s with the excitation wavelength set at 490 nm and emission at 538 nm with a 515-nm cutoff filter in a LS-50B PerkinElmer fluorimeter. Traces were normalized by setting the fluorescence at the initial 15 min stabilization period as 0% and maximal hyperpolarization as −100%.

*Mitochondrial Matrix Calcium and Perifusion*—INS1-E cells ($800 \times 10^5$) were seeded on 15-mm A431 extracellular matrix-coated plastic coverslips. Cells were treated with Ad-GlpK (31) and Ad-CAG-mAeq adenoviruses. The Ad-CAG-mAeq adenovirus was prepared by the method described previously by Miyake *et al.* (37). Briefly, an *Eco*RI fragment that contains the entire aequorin coding sequence fused to the mitochondrial matrix-targeting sequence from human cytochrome *c* oxidase subunit VIII (38) was subcloned into a shuttle vector pAdCAG. The resulting vector pAdCAGmAeq and EcoT22I-digested adenovirus type 5 DNA-terminal protein complex was co-transfected into HEK293 cells. Correctly recombined viral clones were selected by restriction enzyme digestions and purified by CsCl gradient centrifugation. Twenty h after viral treatment, cells were loaded with coelenterazine (2.5 $\mu$M) in (glucose, glutamine, fetal calf serum)-free RPMI 1640 for 1 h and then placed in a hermetically sealed, thermostatted chamber at 37 °C and perifused for 15 min with 2.5 mM glucose KRBH prior to the start of the experiment. The number of emitted photons was measured every second, and effluent fractions were collected for insulin radioimmunoassay at 1-min intervals. Mitochondrial calcium was calculated from the raw photon count data using software available online (www.clocs.com/aequorin/).

## RESULTS

*Glycerol-stimulated Insulin Secretion from Ad-GlpK-treated INS1-E Cells*—The current studies were conducted with the INS1-E cell line, which was clonally selected from the parental INS1 cell line (33) based on its improved insulin secretion profile (39, 40). Static secretion experiments from the INS1-E cells could be conducted over 15-min intervals as opposed to 2–3 h intervals with parental INS-1 cells (31), allowing a more relevant correlation of metabolite levels to secretion.

INS1-E cells engineered for glycerol kinase expression by treatment with the Ad-GlpK adenovirus secrete insulin in a glucose dose-dependent manner with maximal secretion occurring at 10 mM glucose (Fig. 1*A*). Glycerol kinase expression does not affect the glucose dose-response curve since untreated INS1-E cells have a similar profile (41). Ad-GlpK-treated cells are more sensitive to glycerol than glucose such that similar amounts of insulin are secreted in response to 16 mM glucose or 2 mM glycerol (Fig. 1*B*). In addition to glycerol, *Escherichia coli* glycerol kinase (as expressed with the Ad-GlpK virus) phosphorylates DHA to yield the glycolytic intermediate DHAP. DHA is as potent as glycerol in Ad-GlpK-treated cells with maximal stimulation of insulin secretion occurring at 2 mM DHA (Fig. 1*C*). Neither glycerol nor DHA stimulates insulin secretion in control INS1-E cells lacking glycerol kinase overexpression, assuring that phosphorylation and subsequent metabolism of these fuels is required for stimulation of insulin secretion (Fig. 1, *B* and *C*). The lower threshold for stimulation of insulin

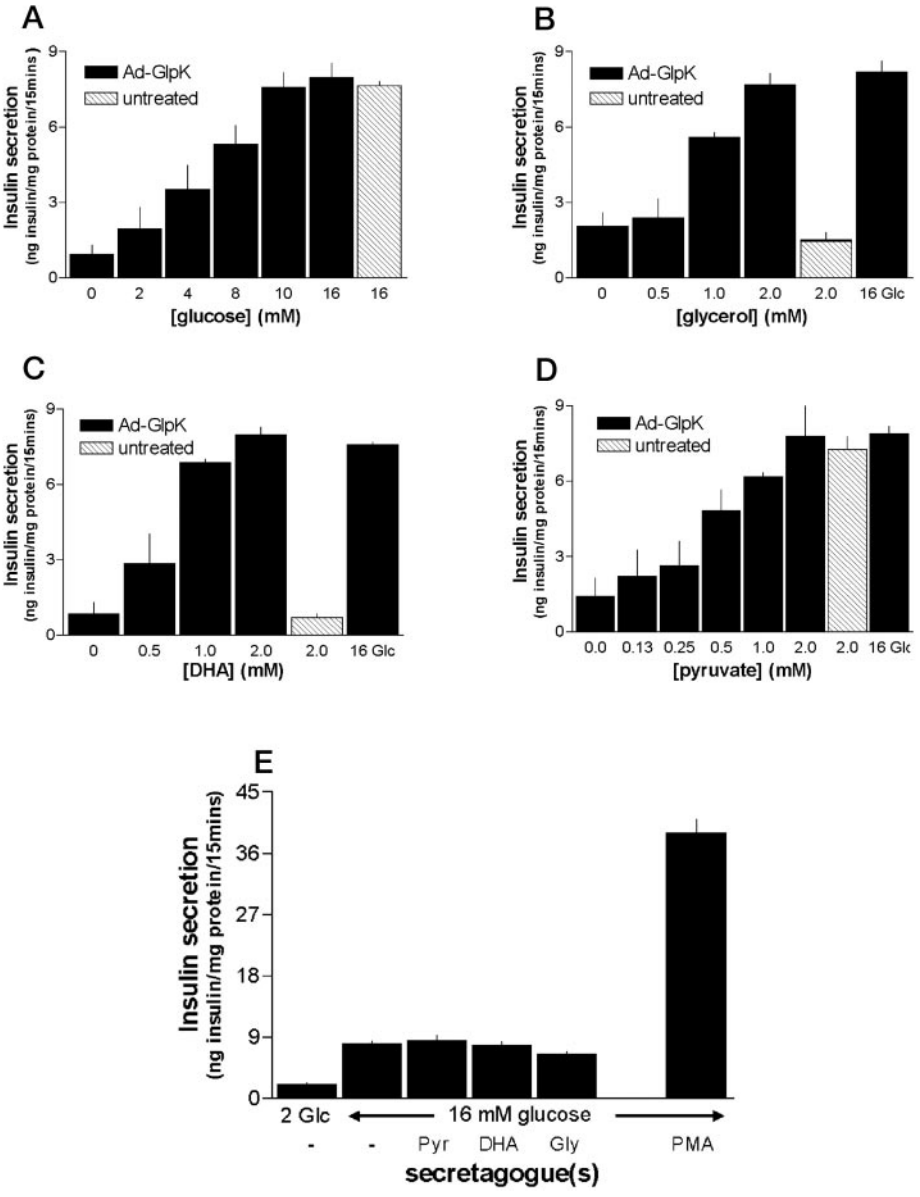


FIG. 1. **Stimulated insulin secretion with four fuel secretagogues.** Insulin release from ~1.5 × $10^6$ INS1-E cells was measured after a 15-min static incubation with the given concentration of each secretagogue. INS1-E cells were treated with (*solid bar*) or without (*hatched bar*) Ad-GlpK adenovirus. Glycerol kinase activity for these experiments was 44.4 ± 3.8 and 0.7 ± 0.2 nmol/mg protein/min for Ad-GlpK-treated and untreated INS1-E cells, respectively ($n$ = 8). *A*, dose-response curve for glucose. Note that glucose reaches maximal stimulation at 10 mM and that Ad-GlpK treatment does not affect the 16 mM glucose response. *B*, dose-response curve for glycerol. Glycerol stimulation attains maximal secretory potency at 2 mM, which is comparable with a 16 mM glucose stimulus. Note that untreated INS1-E cells are not glycerol-responsive. *C*, dose-response curve for DHA. Stimulation of insulin secretion with DHA reaches a maximum at 2 mM, and a similar response is achieved with 16 mM glucose. DHA (2 mM) is ineffective on untreated INS1-E cells. *D*, dose-response curve for pyruvate. Pyruvate stimulation of Ad-GlpK-treated INS1-E cells reaches a maximal limit at 1–2 mM. This stimulation is comparable with a 16 mM glucose challenge, and Ad-GlpK treatment does not affect the magnitude of the pyruvate response. *E*, insulin secretion with secretagogue combinations and PMA. INS1-E cells treated with Ad-GlpK adenovirus were stimulated with combinations of 16 mM glucose (*Glc*) and 2 mM pyruvate (*Pyr*), 2 mM DHA, 2 mM glycerol (*Gly*), or 50 nM PMA. Note that none of the fuel secretagogue combinations could surpass the insulin release of 16 mM glucose alone and the potentiator, PMA, could exceed this limitation by 485%. Each *bar* represents the mean and S.E. of 3–5 experiments performed in 2–6 replicates. *Panels B–D* include a 16 mM glucose control performed on the same cell preparations.

secretion seen with glycerol and DHA as compared with glucose is consistent with the high affinity of glycerol kinase for the triose substrates ($K_m$ = 1.3 μM for glycerol and 500 μM for DHA) (42). In contrast, glucose entry into triose metabolism is restricted by the low affinity glucokinase ($S_{0.5}$ ~8 mM) (43). The similar threshold for stimulation of insulin secretion by glycerol as compared with DHA may seem surprising in light of the higher $K_m$ of glycerol kinase for the DHA. However, to enter glycolysis, glycerol phosphate must first be converted to DHAP by the cytosolic or the $Ca^{2+}$-sensitive mitochondrial glycerophosphate dehydrogenases, which have $K_m$ values of 300 μM (44) and 1–9 mM (45, 46), respectively, for glycerol phosphate, whereas DHAP bypasses this reaction to enter glycolysis.

A fourth fuel secretagogue, pyruvate, was utilized to isolate those coupling factors that are derived from mitochondrial metabolism. Pyruvate has the lowest threshold concentration for stimulation of insulin secretion among the four fuels studied with half-maximal stimulation occurring at 0.5 mM (Fig. 1*D*). Note that all four secretagogues caused a similar rate of insulin secretion at their maximally effective concentrations, and this ceiling could not be exceeded by combinations of the four fuels (Fig. 1*E*). These results suggest that a common limit in metabolism is attained with each of the four fuel stimuli, and this in turn restricts the metabolic signaling of insulin exocytosis. An alternative possibility is that that the ceiling of insulin release is set by steps of exocytosis or insulin biosynthesis. This possibility can readily be ruled out by known potentiators of fuel-stimulated insulin release. As shown in Fig. 1*E*, the inclusion of the phorbol ester, PMA, with 16 mM glucose can surpass the secretory limit imposed by fuel stimuli alone by 485%.

*Comparison of Glycolytic Metabolite Levels for Glucose, Glycerol, DHA, and Pyruvate*—Following 15 min of stimulation with the various fuels and measurement of insulin secretion as shown in Fig. 1, the cells were collected for measurement of the levels of various glycolytic intermediates. Triose phosphate levels (DHAP + GAP) increased 3.3-fold as glucose was raised from 2 to 16 mM (Fig. 2*B*). In comparison, at concentrations with a secretory effect equivalent to the maximally effective doses of glucose, DHA and glycerol caused triose phosphate levels to rise to 3.9 and 5.0 times above those observed at 16 mM glucose, respectively. Predictably, as pancreatic beta cells lack phoshoenolpyruvate carboxykinase (47), 2 mM pyruvate did not increase triose phosphate levels while stimulating insulin secretion to the same extent as the other fuels. It has been suggested that glyceraldehyde phosphate dehydrogenase be-

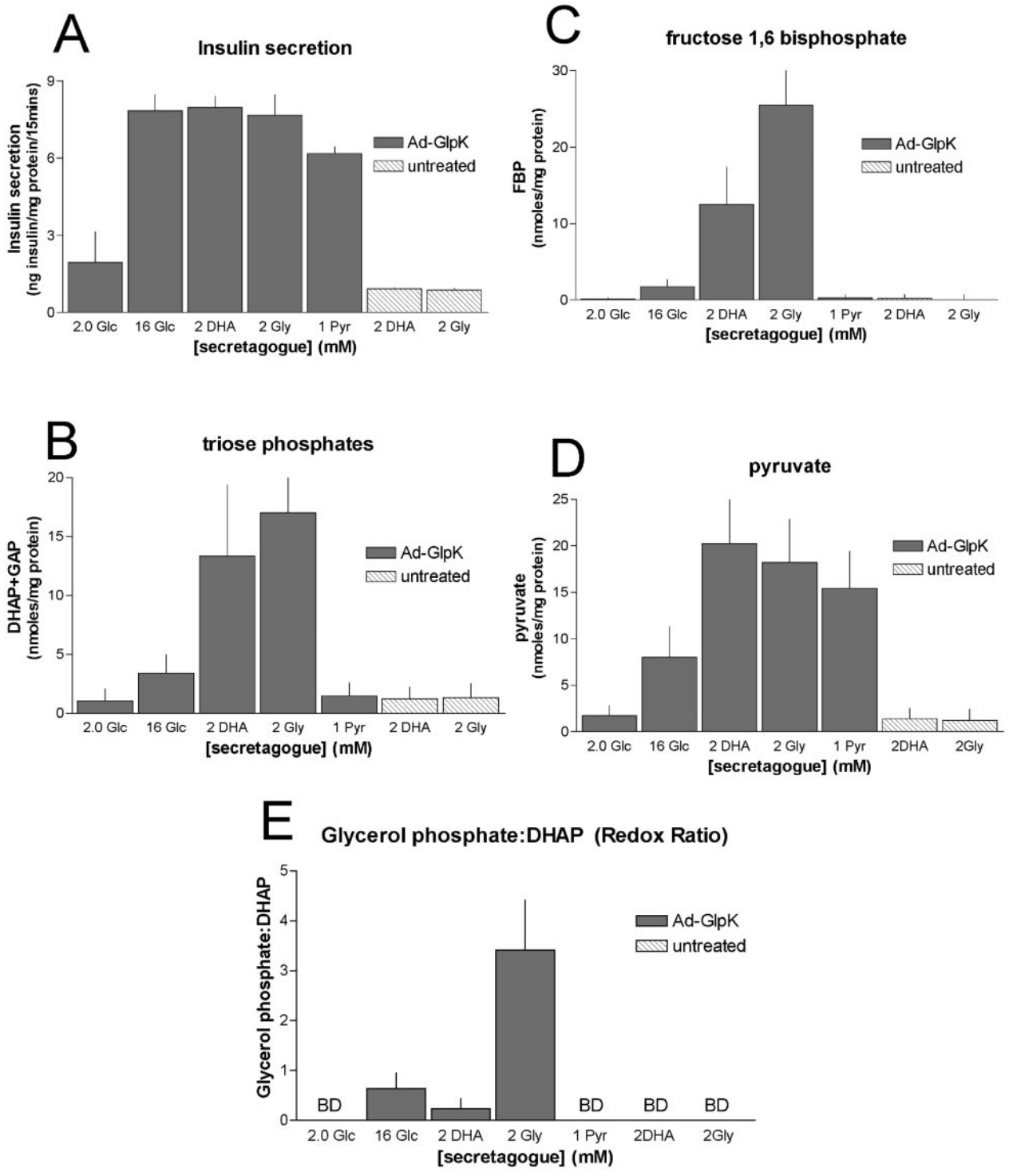


FIG. 2. **Glycolytic intermediate measurements.** Neutralized perchloric acid cellular extracts were prepared from the same samples obtained from the secretion experiments in Fig. 1 and assayed for the following glycolytic intermediates. *A*, fuel-stimulated insulin secretion. This is a summary of selected insulin secretion results from Fig. 1. Note that insulin release stimulated by 16 mM glucose (*Glc*), 2 mM DHA, 2 mM glycerol (*Gly*), and 1 mM pyruvate (*Pyr*) is similar despite marked differences in glycolytic intermediate profiles. *B*, triose phosphates. The combined levels of DHAP and GAP were assayed from cellular extracts. Note that the triose phosphates measured from DHA and glycerol-stimulated Ad-GlpK-treated INS1-E cells greatly exceed those levels obtained in cells receiving a 16 mM glucose stimulus. Pyruvate (1 mM) in Ad-GlpK-treated cells or DHA and glycerol (2 mM) in untreated INS1-E cells do not raise triose phosphate levels above those observed with 2 mM glucose. *C*, fructose 1,6-bisphosphate. FBP levels were drastically elevated by glycerol and DHA (2 mM) relative to a 16 mM glucose stimulation in Ad-GlpK-treated cells. Glycerol increased FBP levels more than DHA, likely due to the exhaustion of cytosolic $NAD^+$ and impairment of GAP disposal via glyceraldehyde phosphate dehydrogenase. Pyruvate (1 mM) in Ad-GlpK-treated cells and DHA and glycerol did not elevate FBP levels above those observed with 2 mM glucose. *D*, pyruvate. A stimulation of both 2 mM trioses and 1 mM pyruvate led to an approximate doubling of pyruvate levels relative to 16 mM glucose after a 15-min challenge. In untreated INS1-E cells, DHA and glycerol did not elevate pyruvate levels above levels observed with 2 mM glucose. *E*, redox ratio. The cytosolic redox state was estimated by splitting the extract into two equal parts and measuring glycerol phosphate and DHAP in each half of the extract. Glycerol phosphate levels were below detection (*BD*) of the assay for 2 mM glucose, 1 mM pyruvate, and in the untreated INS1-E cells challenged with 2 mM DHA and 2 mM glycerol. Note that 2 mM DHA decreases and 2 mM glycerol increases this ratio relative to a 16 mM glucose challenge without an effect on insulin secretion from each of these three stimuli. Each *bar* represents the mean and S.E. of 6–8 experiments.

comes rate-limiting as substrate flux into the distal portion of glycolysis is increased in beta cells and insulinoma cell lines, which is possibly related to the limited capacity for $NAD^+$ regeneration (48, 49). This may in part explain the higher levels of triose phosphates caused by incubation of Ad-GlpK-treated cells with DHA or glycerol relative to glucose. To address this point, fructose 1,6-bisphosphate (FBP) levels were measured as they would be predicted to rise with an accumulation of DHAP and GAP. FBP levels increased 15-fold as glucose was raised from 2 to 16 mM (Fig. 2*C*). However, incubation of Ad-GlpK-treated cells with 2 mM DHA or 2 mM glycerol caused FBP levels to rise 7- and 14-fold higher, respectively, than with 16 mM glucose. The greater accumulation of FBP in the presence of glycerol may be due to the competition for $NAD^+$ between glycerol phosphate dehydrogenase and glyceraldehyde phosphate dehydrogenase. FBP levels did not change in Ad-GlpK-treated cells incubated with 2 mM pyruvate or in untreated cells incubated with 2 mM glycerol or 2 mM DHA relative to basal levels in the same cells incubated with 2 mM glucose.

*Comparison of Pyruvate Levels in Ad-GlpK-treated Cells Incubated with Glucose, Glycerol, DHA, or Pyruvate*—We next measured pyruvate levels in Ad-GlpK-treated cells incubated with each of the four fuels. Stimulation with 16 mM glucose increased pyruvate levels 4.6-fold over levels obtained at 2 mM glucose (Fig. 2*D*). The increase in pyruvate production from 2 mM glycerol and 2 mM DHA was significantly higher than with 16 mM glucose, reaching levels that were 12- and 11-fold higher than 2 mM glucose. This observation further demonstrates that triose substrates enter the distal portion of glycolysis more efficiently than glucose, which is constrained by the high $K_m$ value of glucokinase. In our prior study, lactate (measured in the secretion medium) was 2–3-fold higher in Ad-GlpK-treated cells incubated with glycerol relative to glucose (31). This enhanced capacity for lactate production from glycerol was hypothesized to result from high NADH levels caused by flux through cytosolic glycerol phosphate dehydrogenase. In the current study, intracellular lactate levels were measured, and we confirm an increased capacity of lactate production from glycerol as compared with glucose (84.4 ± 11.4 *versus* 51.8 ± 12.0 nmol/mg protein/15 min) at 2 mM glycerol and 16 mM glucose, respectively ($n = 3$) Interestingly, 2 mM DHA also causes a large increase in lactate levels (120 ± 20.2 nmol/mg protein/15 min) despite the fact that DHA bypasses NADH generation at the glycerophosphate dehydrogenase step. These results suggest that the large increment in lactate output that occurs in cells incubated with either triose fuel is probably a direct consequence of elevated pyruvate levels rather than a function of redox conditions.

*Comparision of Redox Conditions in Ad-GlpK-treated Cells Incubated with Glucose, Glycerol, DHA, or Pyruvate*—In INS1-E cells with glycerol kinase expression, both DHA and glycerol stimulate insulin secretion even though their phosphorylated products lie on opposite sides of the glycerol phosphate dehydrogenase reaction. Measurements of certain redox pairs (such as glycerol phosphate:DHAP) are a reflection of the cellular redox state (50). We therefore investigated the role of redox status by measurement of the relative levels of glycerol phosphate and DHAP in cells incubated with the various fuels. The redox ratio (glycerol phosphate:DHAP) in cells stimulated with 16 mM glucose for 15 min was 0.64 ± 0.31 (Fig. 2*E*). Following treatment with 2 mM DHA, the redox ratio was lower (0.23 ± 0.21), whereas treatment with 2 mM glycerol caused it to be 5.3 times higher (3.4 ± 1.0) than observed with 16 mM glucose. Despite the extreme shift in redox state that it causes, glycerol is as effective a secretagogue as glucose and DHA (Fig. 2*A*), strongly suggesting that cytosolic redox conditions are not a key factor in stimulation of insulin secretion by carbohydrate fuels. Note that due to the low levels of glycerol phosphate in INS1-E cells treated with 2 mM glucose or 1 mM pyruvate, the ratios under these conditions could not be accurately determined.

*Mitochondrial Oxidation of Glycerol and DHA*—To this point, increased pyruvate levels is the common denominator for all of the tested fuel secretagogues. Due to the lack of phoshoenolpyruvate carboxykinase (23) activity in beta cells, this suggests that the potency of a given fuel is determined by pyruvate entry into the mitochondria and its subsequent metabolism. The fact that the triose secretagogues can increase pyruvate and lactate levels beyond those observed from a glucose stimulus further suggests that mitochondrial metabolism limits the disposal of pyruvate. To substantiate this, we measured oxidation of 2-$^{14}$C-labeled glycerol or DHA in Ad-GlpK-treated INS1-E cells. The $^{14}$C label at carbon 2 is lost to $CO_2$ either at the $\alpha$-ketoglutarate dehydrogenase step of the tricarboxylic acid cycle when pyruvate enters via pyruvate dehydrogenase or at either the $\alpha$-ketoglutarate or isocitrate dehydrogenase reactions when pyruvate enters the tricarboxylic acid cycle via pyruvate carboxylase. The 2-$^{14}$C-labeled substrates were selected over the U-$^{14}$C-labeled substrates used in our previous study (31) to allow a more precise determination of the flux through these two tricarboxylic acid cycle dehydrogenases. As shown in Fig. 3, oxidation of [2-$^{14}$C]glycerol or DHA in Ad-GlpK-treated cells increased in a dose-dependent manner, reaching a maximum for both fuels at a concentration of 2 mM, which is in close correlation with insulin secretion. 2-$^{14}$C oxidation for both fuels was blocked by 50 nM rotenone (an inhibitor of NADH-coenzyme Q oxidoreductase of the electron transport chain). [2-$^{14}$C]Glycerol oxidation was negligible in untreated INS1 cells, whereas oxidation was measurable at 2 mM DHA, albeit not at a rate sufficient to stimulate insulin secretion.

Since each of the fuel stimuli used in this study generates pyruvate, it is possible that mitochondrial transport and metabolism of pyruvate is the common constraint of metabolism. To address this possibility, we measured [1-$^{14}$C]pyruvate oxidation at various pyruvate concentrations. The 1-$^{14}$C label is removed as $CO_2$ as pyruvate dehydrogenase catalyzes the decarboxylation of pyruvate to acetyl-CoA. Pyruvate concentrations above 1 mM neither increase oxidation (Fig. 3*B*) nor enhance insulin secretion (Fig. 1*D*). Pyruvate dehydrogenase does not likely have excess capacity in intact cells since the pyruvate concentration to achieve maximal [1-$^{14}$C]pyruvate oxidation was not greater than the concentration to maximally stimulate insulin secretion.

*Hyperpolarization of Mitochondrial Membrane Potential by Glycerol, DHA, Pyruvate, and Glucose*—To evaluate possible metabolic constraints imposed by the electron transport chain and the generation of a proton gradient, mitochondrial membrane potential was measured using the fluorescent dye rhodamine-123. Fuel oxidation via the tricarboxylic acid cycle supplies NADH and $FADH_2$ to power the formation of a proton gradient across the inner mitochondrial membrane. This proton gradient in turn provides the energy to drive ATP formation. In concert with the formation of the gradient, the inner mitochondrial membrane becomes hyperpolarized due to the extrusion of positively charged protons. As observed with substrate oxidation, 2 mM glycerol had no effect on mitochondrial activation in untreated INS1-E cells (Fig. 4*A*), whereas in the same cells, 16 mM glucose caused a clear hyperpolarization and 2 mM DHA was about 15% as effective as glucose. In Ad-GlpK-treated INS1-E cells, an initial stimulation with either 2 mM

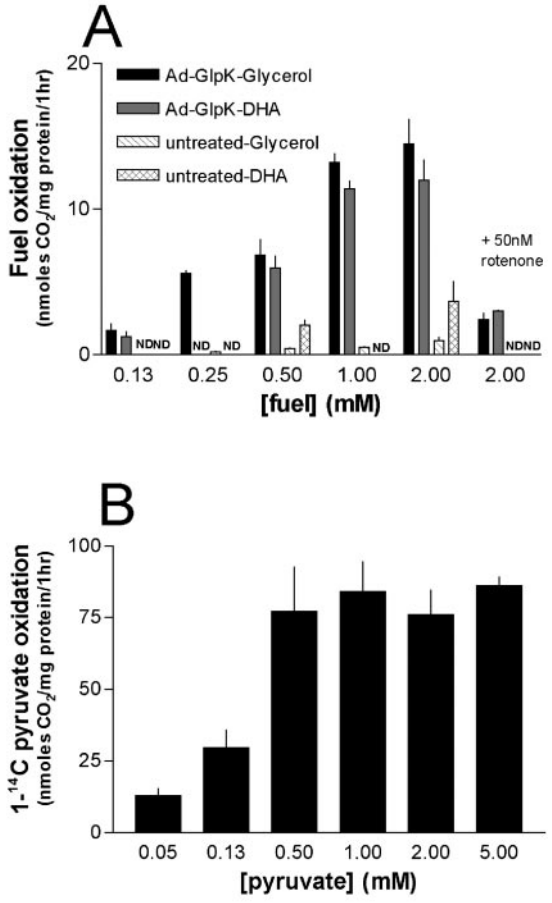


FIG. 3. **Triose and pyruvate oxidation.** *A*, triose oxidation. $CO_2$ generation from [2-$^{14}$C]glycerol or [2-$^{14}$C]DHA oxidation at the given substrate concentrations was measured after 1 h from INS1-E cells treated with (*solid bars*) or without (*hatched bars*) Ad-GlpK adenovirus. Ad-GlpK adenovirus enables efficient oxidation of DHA and glycerol relative to untreated INS1-E cells at all tested concentrations. Although significantly higher triose oxidation was observed at 0.5 mM in Ad-GlpK-treated *versus* untreated INS1-E cells, this increase was not accompanied by a stimulation of insulin secretion (see Fig. 1). Note that in untreated cells, there is a general trend of a more efficient oxidation of DHA as compared with glycerol. Rotenone (50 nM) blocked oxidation of both DHA and glycerol (at 2 mM) by 80% in Ad-GlpK-treated INS1-E cells. Each *bar* represents the mean and S.E. of 3–7 experiments performed in triplicate. *ND*, not determined. *B*, pyruvate oxidation. $CO_2$ generation from [1-$^{14}$C]pyruvate oxidation at the given concentrations was measured after 1 h from INS1-E cells. Each *bar* represents the mean and S.E. of 3 experiments performed in triplicate.

glycerol (Fig. 4*A*) or 2 mM DHA (Fig. 4*B*) hyperpolarized the mitochondrial membrane to a point at which subsequent addition of 16 mM glucose had no further effect. This suggests that 2 mM triose is sufficient to maximally stimulate the respiratory chain. This tight relationship of mitochondrial membrane potential and insulin secretion is further supported by dose-response studies performed with all four fuels, wherein maximal activation of mitochondrial membrane potential (Fig. 4, *C* and *D*) and maximal activation of insulin secretion (Fig. 1) were correlated in each case.

Succinate bypasses NADH-oxidoreductase (site I) and provides electrons to the electron transport chain via the FAD-linked succinate dehydrogenase (site II). Methyl succinate, a plasma membrane-permeant source of succinate, hyperpolarizes the mitochondrial membrane in a dose-dependent fashion (data not shown), although the maximal effect obtained (at 5 mM) is only 50% of a 16 mM glucose stimulation (Fig. 4*E*). Methyl succinate (5 mM) does not cause a further hyperpolarization when following a glucose (Fig. 4*E*), triose, or pyruvate stimulus (data not shown). Again, this suggests that the maximal proton gradient attained with each fuel cannot be surpassed even when providing electron input beyond NADH-oxidoreductase.

*Time Course of Insulin Secretion and Mitochondrial $Ca^{2+}$*—The foregoing studies were largely carried out under static incubation conditions. To assess mitochondrial activation in perifused INS1-E cells in real time, cells were treated with two adenoviruses, one encoding a mitochondrial targeted aequorin (Ad-CAG-mAeq), a luminescent $Ca^{2+}$ sensor, and the Ad-GlpK virus. This system allows simultaneous evaluation of mitochondrial matrix $Ca^{2+}$ (which reflects the activation of mitochondria) and insulin release in response to the various fuels (51). Cells prepared in this manner were perifused without glucose for 15 min prior to a 10-min stimulation with DHA. A sharp increase in mitochondrial $Ca^{2+}$ occurred within 30–60 s of DHA application, followed 30–60 s later by a surge in insulin secretion (Fig. 5*A*). Switching back to perifusion medium without DHA returned both mitochondrial calcium and insulin output to basal levels. After 30 min, a restimulation with 16 mM glucose caused increases in both mitochondrial calcium and insulin secretion that were almost identical in temporal sequence and magnitude as observed with 2 mM DHA. Similar results were obtained with 2 mM glycerol. (Fig. 5*B*). Neither DHA nor glycerol elevated mitochondrial $Ca^{2+}$ or stimulated insulin secretion in INS1-E cells treated only with the Ad-CAG-mAeq adenovirus (data not shown). To verify that glycerol-stimulated insulin secretion requires mitochondrial respiration, 50 nM rotenone was shown to suppress both the mitochondrial $Ca^{2+}$ signal and insulin secretion induced by 2 mM glycerol (Fig. 5*C*).

Combined with the dynamic measurements of mitochondrial membrane potential (Fig. 4), these experiments define the following temporal sequence. Approximately 3 min after fuel application, the mitochondrial membrane becomes maximally hyperpolarized (Fig. 4, *A* and *B*). Two min later ($t$ = 5 min), mitochondrial $Ca^{2+}$ peaks, and an additional 2 min thereafter ($t$ = 7 min), insulin secretion reaches a maximum. Mitochondrial membrane hyperpolarization therefore precedes the elevation of mitochondrial matrix $Ca^{2+}$ and insulin secretion, suggesting that this event plays a primary role in the regulation of fuel responsiveness.

## DISCUSSION

By investigating the metabolic fates of glycerol, DHA, glucose, and pyruvate, our data suggest that mitochondrial activation is the common point of action of each of these fuels. Large increases of glycolytic intermediates did not impact insulin secretion, whereas mitochondrial membrane hyperpolarization strongly correlated with the limitations of insulin output. Expression of *E. coli* glycerol kinase enables phosphorylation of DHA and glycerol with their phosphorylated products lying on opposite sides of the glycerol phosphate shuttle. Very large alterations in the ratio of DHAP:glycerol phosphate (indicative of redox status) did not impact insulin secretion as long as further mitochondrial metabolism was allowed. In contrast, blocking the respiratory chain with rotenone inhibited insulin secretion in response to any of the four fuels. Rotenone specifically inhibits the respiratory chain at complex I (where NADH generated by several dehydrogenase reactions is oxidized) while leaving the remaining steps of the electron transport chain intact. This property is particularly advantageous when understanding glycerol stimulation of insulin secretion. Since cytosolic glycerol phosphate can directly produce $FADH_2$ in the mitochondria via the mitochondrial FAD-linked glycerophosphate dehydrogenase, metabolism of glycerol can provide input into the electron transport chain downstream of a complex I block. Nonetheless, glycerol responsiveness in INS1-E

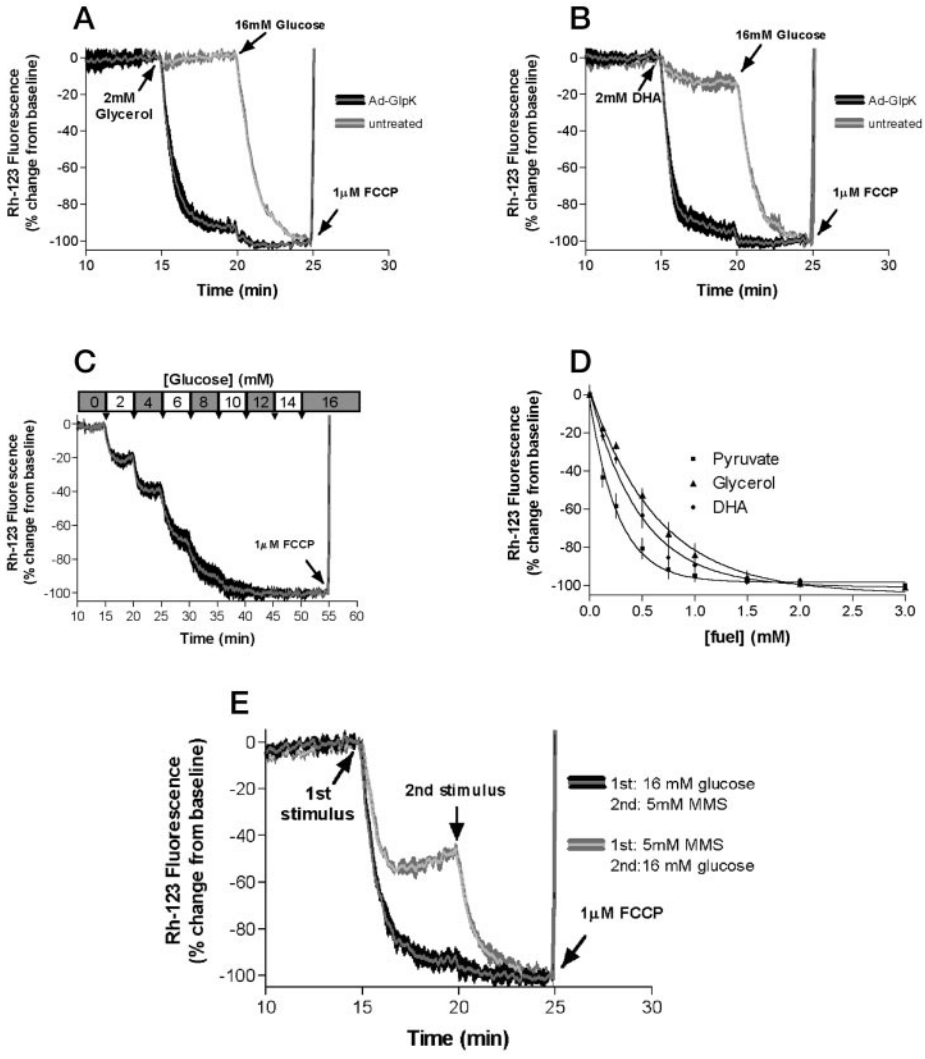


FIG. 4. **Mitochondrial membrane potential.** Fuel-mediated changes in mitochondrial membrane potential were estimated by rhodamine-123 fluorescence. *A*, glycerol-stimulated hyperpolarization. At 15 min, 2 mM glycerol was added followed by 16 mM glucose at 20 min. Note that glycerol hyperpolarizes the mitochondrial membrane only in Ad-GlpK-treated INS1-E cells and that 16 mM glucose does not markedly enhance this effect further. *B*, DHA-stimulated hyperpolarization. At 15 min, 2 mM DHA was added followed by 16 mM glucose at 20 min. Note that DHA slightly hyperpolarizes the mitochondrial membrane in untreated INS1-E cells and hyperpolarizes Ad-GlpK-treated INS1-E cells to the same extent as 16 mM glucose. *C*, glucose-stimulated hyperpolarization. At 5 min intervals, additions of glucose in 2 mM increments were added to the cell suspension until a concentration of 16 mM was reached. Complete hyperpolarization occurs at 10 mM glucose. *D*, dose-dependence of pyruvate, glycerol, and DHA. ■, pyruvate; ▲, glycerol; ●, DHA. Sequential additions of each fuel were added until a maximal hyperpolarization was obtained. Once this maximum hyperpolarization was reached, no combination of any of the fuel secretagogues could surpass this limit (data not shown). Note the left shift in the concentration dependence of pyruvate as compared with the triose-secretagogues. Each data point represents the mean and S.E. of 3–4 determinations at the given concentration. *E*, mono-methyl succinate (*MMS*)-stimulated hyperpolarization. At 15 and 20 min, either 5 mM mono-methyl succinate was followed by 16 mM glucose or 16 mM glucose was followed by 5 mM MMS. Note that MMS could maximally attain only 50% of a glucose stimulus and that when combined, these fuels cannot exceed a 16 mM glucose hyperpolarization. For *panels A–C* and *E*, each trace represents the mean and S.E. of 3–4 experiments. At the end of each trace, 1 μM FCCP was added to uncouple the mitochondria and plateaued at similar levels for each trace (not shown).

cells requires NAD-substrate oxidation as evident by the impairment of insulin secretion by rotenone (Fig. 5*C*). This observation demonstrates that the glycerophosphate shuttle alone cannot sustain insulin secretion without an ability to provide electron input at complex I and regenerate $NAD^+$.

Although pyruvate is an effective stimulus in the INS1 cell line, pyruvate-stimulated insulin secretion is not typically observed in pancreatic islet preparations. This observation is the basis of the pyruvate paradox, because pyruvate oxidation is observed in such preparations but is not accompanied by insulin secretion (20, 21). This has been partially addressed by the finding of low levels of expression of MCT-1, a plasma membrane pyruvate transporter, in rat islets as compared with the INS1 cell line (52). This report also demonstrated that adenovirus-mediated expression of MCT-1 confers pyruvate-stimulated insulin secretion in rat islets. Pyruvate oxidation in islets in the absence of MCT-1 expression has been suggested to occur in non-beta bells. In support of this idea, immunofluorescence studies suggest that MCT-1 expression is concentrated at the periphery of the rat islet where most of the non-beta cells reside (53). However, the authors also report low levels of MCT-1 expression in non-beta cells by immunoblot analysis, suggesting that further investigation of this issue will be required.

Nonetheless, the fact that pyruvate is an effective secretagogue in a cell type that lacks gluconeogenic enzymes and has poor lipogenic capacity suggests that mitochondrial metabolism of pyruvate is the major means for generation of coupling factors. Consistent with this idea, neither triose phosphates nor FBP increase during pyruvate stimulation (Fig. 2, *B* and *C*), whereas mitochondrial depolarization (Fig. 4*D*) is strongly

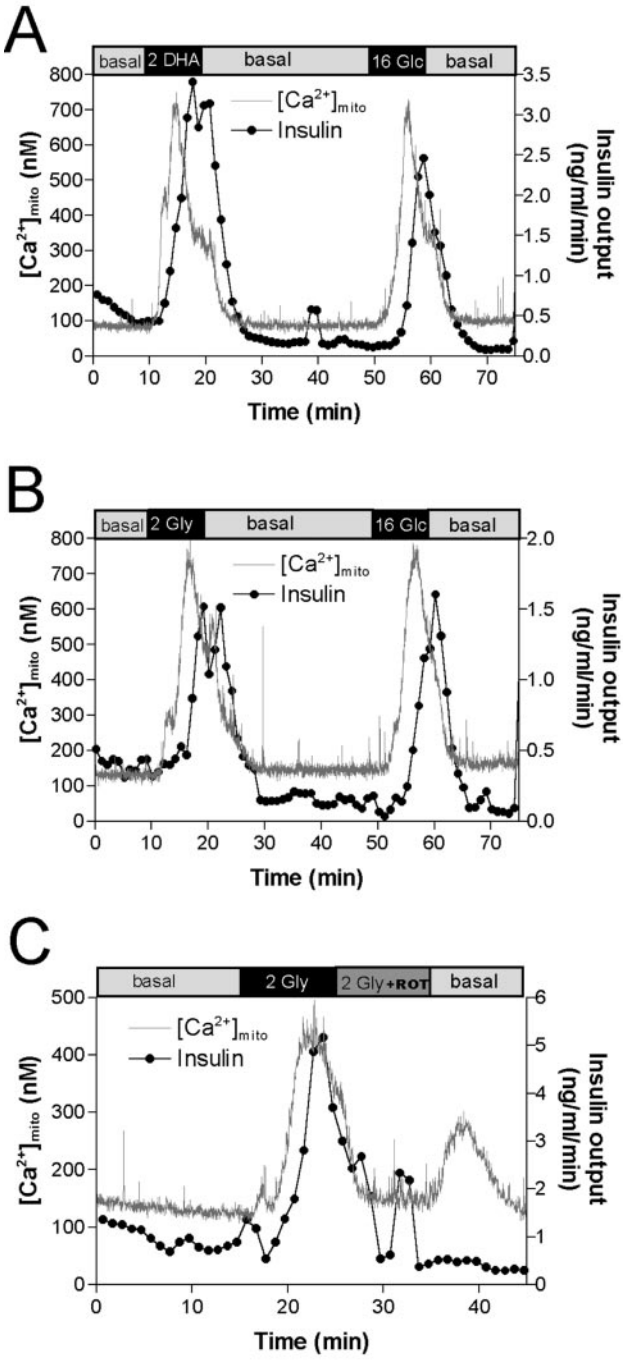


FIG. 5. **Mitochondrial calcium and insulin secretion.** Simultaneously, emitted photons were measured (1-s intervals) and perifusate was collected (1-min intervals) from INS1-E cells perifused with several media changes. The mitochondrial $Ca^{2+}$ levels were calculated from the photon emission of coelenterazine-loaded mAeq expressing INS1-E cells. Insulin was measured in the perifusate by radioimmunoassay. *A*, DHA stimulation. Following a 15-min perifusion of KRBH with 2.5 mM glucose (*Glc*), the medium was switched to basal medium (KRBH without glucose) for 5 min, after which the collection of photon count data and perifusate was begun. After an additional 10-min perifusion of basal medium, a 10-min stimulus with 2 mM DHA was initiated followed by 30 min with basal medium, a second 10-min stimulation with 16 mM glucose, and a final 15-min of basal medium. Note that the kinetics and magnitude of DHA and glucose stimulation are similar. *B*, glycerol (*Gly*) stimulation. The protocol of *panel A* was repeated with 2 mM glycerol replacing the 2 mM DHA stimulation. Again, the kinetics and magnitude of glycerol and glucose stimuli are similar. *C*, rotenone (*ROT*) inhibition of glycerol stimulation. After a 10-min stimulation with 2 mM glycerol, 50 nM rotenone (an inhibitor of NAD-linked substrate oxidation) rapidly decreased both mitochondrial $Ca^{2+}$ and insulin release. Each trace is representative of 3–5 experiments.

induced and correlates with insulin secretion (Fig. 1*D*). Pyruvate has two immediate fates upon entering the mitochondria, decarboxylation by pyruvate dehydrogenase to yield acetyl CoA and carboxylation by pyruvate carboxylase to yield oxaloacetate. Pancreatic beta cells have high pyruvate carboxylase activity as compared with other non-gluconeogenic tissues (54, 55). One advantage of high pyruvate carboxylase activity is the provision of tricarboxylic acid cycle intermediates. Specifically, and increase in oxaloacetate facilitates efficient entry of acetyl CoA into the tricarboxylic acid cycle and provides substrate for the pyruvate malate and malate aspartate shuttles. Likewise, citrate is utilized by the pyruvate citrate shuttle, and $\alpha$-ketoglutarate serves as substrate for glutamate synthesis (40).

Pyruvate and triose fuels bypass the primary flux determining enzyme of glycolysis, glucokinase, and thus reveal metabolic constraints beyond this step. Other studies have demonstrated a similar observation by reducing the control strength of glucokinase by overexpression of glucokinase. With a mere 2.5-fold increase in glucokinase activity in an INS clone engineered for inducible expression of glucokinase, the rate of insulin secretion at 6 mM glucose increased from 43 to 84% of a 12 mM glucose challenge (56). However, the maximal insulin output achieved at 12 mM glucose was not enhanced by increased glucokinase activity. Similarly, a 20-fold increase of glucokinase activity by adenoviral-mediated expression of glucokinase in rat pancreatic islets only increased insulin output by 29%, again indicating factors downstream of glucokinase restrict metabolism (57).

In this study, we suggest that the ultimate limitation of beta cell metabolism is the formation of the proton gradient since the secretory potency of each of the fuels used in this study converge on their stimulatory effects on mitochondrial membrane potential. The proton gradient in turn directly limits other metabolic steps including pyruvate entry into the mitochondria (58) and the NAD+ regeneration required for sustaining the activity of mitochondrial dehydrogenases. The possibility that pyruvate entry becomes limited is supported by the observation that triose secretagogues can increase pyruvate levels above those observed from a glucose stimulus (Fig. 2*D*). Bypassing NADH-oxidoreductase with either the excess glycerol phosphate generated during a glycerol stimulus in GlpK-expressing INS1-E cells (Fig. 4*A*) or methyl succinate (Fig. 4*E*) did not further hyperpolarize the mitochondrial membrane. This observation strongly suggests that complex I of the electron transport chain does not in itself limit the formation of the proton gradient, but rather the rate of the gradient formation exceeds the dissipation rate under these conditions.

It must be clarified that although our results demonstrate a common constraint in metabolism and fuel-stimulated insulin secretion, they do not suggest that with the highest concentration of each fuel tested here, the absolute limit of insulin output was obtained. Clearly, potentiators such as fatty acids, incretin hormones, and phorbol esters (59–61) can surpass the limits of a fuel-only stimulus, and this observation is similarly demonstrated in this study (Fig. 1*E*). This implies that the efficacy of a fuel-only stimulus is limited by mitochondrial metabolism and not by the innate secretory capacity of the cell.

The mechanism underlying the limitations imposed by the mitochondrial membrane potential is likely related to the thermodynamics of generation of the proton gradient across the mitochondrial inner membrane. NADH and $FADH_2$ generated in the tricarboxylic acid cycle donate electrons to the electron transport chain, which in turn supplies the energy to pump protons across the mitochondrial inner membrane at three distinct sites (complexes I, III, and IV) to create a gradient. The energy required to pump a proton across this gradient in-

creases as the pH difference between compartments increases. This energy requirement is further increased because the internal surface of the inner mitochondrial membrane becomes more negative than its external surface as each proton is pumped out of the matrix. These two factors cause the energy required for creating the proton gradient to increase exponentially with each additional proton pumped out of the mitochondrial matrix. Eventually the maximal proton gradient will be reached when the energy required to pump protons exceeds the energy provided by the reduction potential of NADH and $FADH_2$, and proton pumping will cease. The limitations of the formation of the proton gradient therefore limit the production of mitochondrial coupling factors such as ATP. In addition to ATP/ADP exchange, the mitochondrial membrane potential drives the transport of other metabolites between mitochondrial and cytosolic compartments. Again, of particular interest is glutamate/aspartate exchange (62) given that glucose-derived glutamate may act directly upon insulin secretion (40).

The importance of generation of a proton gradient in secretion coupling is further supported by data showing that inhibitors of the electron transport chain and ATP generation or agents that dissipate the proton gradient all impair insulin secretion. The uncoupling proteins (UCP1–3) dissipate the energy of the protein gradient as heat rather than ATP generation by facilitating proton transfer across the inner mitochondrial membrane (63). Overexpression of UCP2 in normal rat islets decreases ATP content (64) and inhibits GSIS (65). Induction of UCP2 by chronic exposure of cells to fatty acids (66), feeding rodents with a high fat diet (64), or the up-regulation of UCP2 found in *ob*/*ob* mouse islets is accompanied in all cases with a defect in fuel-stimulated secretion. Conversely, UCP2-deficient mice *UCP2* (−/−) demonstrate increased ATP production and improved insulin secretion (67). The resulting *ob*/*ob*, *UCP2* (−/−) mice created from mating these two mouse strains have partially restored glucose sensing, which again highlights the importance of a tight coupling of metabolism to the proton gradient, mitochondrial membrane potential, and ATP generation (66).

We propose that the formation of the mitochondrial proton gradient sets the maximal limit of insulin secretion observed by the four fuels studied here. The implication of this hypothesis is that strategies designed to improve the maximal insulin output will be restricted by this biophysical limitation. Considering that increased insulin output can compensate for insulin resistance in some forms of diabetes, determinants of maximal insulin output may be important targets for new therapeutic approaches. Successful beta cell adaptation to insulin resistance includes increasing beta cell mass via hypertrophy and/or hyperplasia and improved responsiveness (68). Improved fuel responsiveness is generally restricted to an increase in the sensitivity of the fuel rather than improved maximal output. Therefore, strategies that act upon the targets of potentiators and improve the energy conversion from the mitochondrial proton gradient are most likely to improve beta cell performance.

*Acknowledgments*—We thank D. Nappey and O. Dupont for expert technical assistance and Dr. P. Maechler for stimulating discussion. We owe a special thanks to Dr. J. Denis McGarry for instigating our glycerol kinase overexpression studies. His mentorship (to P. A. A. and C. B. N.) and scientific excellence will be remembered and cherished.

REFERENCES

1. Newgard, C. B., and McGarry, J. D. (1995) *Annu. Rev. Biochem.* **64,** 689–719
2. Panten, U., Schwanstecher, M., Wallasch, A., and Lenzen, S. (1988) *Naunyn-Schmiedeberg's Arch. Pharmacol.* **338,** 459–462
3. Detimary, P., Van den Berghe, G., and Henquin, J. C. (1996) *J. Biol. Chem.* **271,** 20559–20565
4. Henquin, J. C. (2000) *Diabetes* **49,** 1751–1760
5. MacDonald, M. J. (1982) *Arch. Biochem. Biophys.* **213,** 643–649
6. MacDonald, M. J. (1995) *J. Biol. Chem.* **270,** 20051–20058
7. Malaisse, W. J., Malaisse-Lagae, F., and Sener, A. (1982) *Endocrinology* **111,** 392–397
8. Giroix, M. H., Baetens, D., Rasschaert, J., Leclercq-Meyer, V., Sener, A., Portha, B., and Malaisse, W. J. (1992) *Endocrinology* **130,** 2634–2640
9. Sener, A., and Malaisse, W. J. (1992) *J. Biol. Chem.* **267,** 13251–13256
10. MacDonald, M. J. (1981) *J. Biol. Chem.* **256,** 8287–8290
11. Mertz, R. J., Worley, J. F., Spencer, B., Johnson, J. H., and Dukes, I. D. (1996) *J. Biol. Chem.* **271,** 4838–4845
12. Eto, K., Tsubamoto, Y., Terauchi, Y., Sugiyama, T., Kishimoto, T., Takahashi, N., Yamauchi, N., Kubota, N., Murayama, S., Aizawa, T., Akanuma, Y., Aizawa, S., Kasai, H., Yazaki, Y., and Kadowaki, T. (1999) *Science* **283,** 981
13. Eto, K., Suga, S., Wakui, M., Tsubamoto, Y., Terauchi, Y., Taka, J., Aizawa, S., Noda, M., Kimura, S., Kasai, H., and Kadowaki, T. (1999) *J. Biol. Chem.* **274,** 25386–25392
14. Malaisse, W. J., Hutton, J. C., Kawazu, S., Herchuelz, A., Valverde, I., and Sener, A. (1979) *Diabetologia* **16,** 331–341
15. MacDonald, M. J., and Fahien, L. A. (1990) *Arch. Biochem. Biophys.* **279,** 104–108
16. Silva, J. P., Kohler, M., Graff, C., Oldfors, A., Magnuson, M. A., Berggren, P. O., and Larsson, N. G. (2000) *Nat. Genet.* **26,** 336–340
17. Rotig, A., Bonnefont, J. P., and Munnich, A. (1996) *Diabetes Metab.* **22,** 291–298
18. Soejima, A., Inoue, K., Takai, D., Kaneko, M., Ishihara, H., Oka, Y., and Hayashi, J. I. (1996) *J. Biol. Chem.* **271,** 26194–26199
19. Kennedy, E. D., Maechler, P., and Wollheim, C. B. (1998) *Diabetes* **47,** 374–380
20. Sener, A., Kawazu, S., Hutton, J. C., Boschero, A. C., Devis, G., Somers, G., Herchuelz, A., and Malaisse, W. J. (1978) *Biochem. J.* **176,** 217–232
21. Zawalich, W. S., and Zawalich, K. C. (1997) *J. Biol. Chem.* **272,** 3527–3531
22. Ashcroft, S. J., Weerasinghe, L. C., and Randle, P. J. (1973) *Biochem. J.* **132,** 223–231
23. Alcazar, O., Gine, E., Qiu-Yue, Z., and Tamarit-Rodriguez, J. (1995) *Biochem. J.* **310,** 215–220
24. Malaisse, W. J., Herchuelz, A., Levy, J., Sener, A., Pipeleers, D. G., Devis, G., Somers, G., and Obberghen, E. V. (1975) *Mol. Cell. Endocrinol.* **4,** 1–12
25. MacDonald, M. J. (1989) *Arch. Biochem. Biophys.* **270,** 15–22
26. Elliot, A. C., Trebilock, R., Yates, P., and Best, L. (1993) *Eur. J. Biochem.* **213,** 359–365
27. Arkhammar, P., Berggren, P. O., and Rorsman, P. (1986) *Biosci. Rep.* **6,** 355–361
28. Juntli-Berggren, L., Rorsman, P., Siffert, W., and Berggren, P. O. (1992) *Biochem. J.* **287,** 59–66
29. Jijkali, H., Nadi, A. B., Cook, L., Best, L., Sener, A., and Malaisse, W. J. (1996) *Arch. Biochem. Biophys.* **355,** 245–257
30. Lembert, N., Joos, H. C., Idahl, L., Ammon, H. P. T., and Wahl, M. A. (2001) *Biochem. J.* **35,** 345–350
31. Noel, R. J., Antinozzi, P. A., McGarry J. D., and Newgard, C. B. (1997) *J. Biol. Chem.* **172,** 18621–18627
32. Skelly, R. H., Wicksteed, B., Antinozzi, P. A., and Rhodes, C. J. (2001) *Diabetes* **50,** 1791–1798
33. Asfari, M., Janjic, D., Meda, P., Li, G., Halban, P. A., and Wollheim, C. B. (1992) *Endocrinology* **130,** 167–178
34. Bergmeyer, H. U. (1974) *Methods of Enzymatic Analysis,* Verlag Chemie GmbH, Weinheim, Germany
35. Antinozzi, P. A., Segall, L., Prentki, M., McGarry, J. D., and Newgard, C. B. (1998) *J. Biol. Chem.* **273,** 16146–16154
36. Wieland, O., and Suyter, M. (1957) *Biochem. Z.* **329,** 320
37. Miyake, S., Makimura, M., Kanegae, Y., Harada, S., Sato, Y., Takamori, K., Tokuda, C., and Saito, I. (1996) *Proc. Natl. Acad. Sci. U. S. A.* **93,** 1320–1324
38. Kennedy, E. D., Rizzuto, R., Theler, J. M., Pralong, W. F., Bastianutto, C., Pozzan, T., and Wollheim, C. B. (1996) *J. Clin. Invest.* **98,** 2524–2538
39. Janjic, D., Maechler, P., Sekine, N., Bartley, C., Annen, A., and Wollheim, C. B. (1999) *Biochem. Pharmacol.* **57,** 639–648
40. Maechler, P., and Wollheim, C. B. (1999) *Nature* **402,** 685–689
41. Maechler P., Antinozzi P. A., and Wollheim, C. B. (2000) *IUBMB Life* **50,** 27–31
42. Hayashi, S., and Lin, E. C. C. (1967) *J. Biol. Chem.* **242,** 1030–1035
43. Matschinsky, F. M., Glaser, B., and Magnuson, M. A. (1998) *Diabetes* **47,** 307–315
44. McGinnis, J., and DeVellis, J. (1974) *Biochim. Biophys. Acta* **364,** 17–27
45. Garrib, A., and McMurray, W. C. (1986) *J. Biol. Chem.* **261,** 8042–8048
46. Rutter, G. A., Pralong, W. F., and Wollheim, C. B. (1992) *Biochim. Biophys. Acta* **1175,** 107–113
47. MacDonald, M. J., McKenzie, D. I., Walker, T. M., and Kaysen, J. H. (1992) *Horm. Metab. Res.* **24,** 158–160
48. Meglasson, M. D., and Matschinsky, F. M. (1986) *Diabetes Metab. Rev.* **2,** 163–214
49. Berman, H. K., and Newgard, C. B. (1998) *Biochemistry* **37,** 4543–4552
50. Matschinsky, F. M., Ghosh, A. K., Meglasson, M. D., Prentki, M., June, V., and von Allman, D. (1986) *J. Biol. Chem.* **261,** 14057–14061
51. Maechler, P., Kennedy, E. D., Pozzan, T., and Wollheim, C. B. (1997) *EMBO J.* **16,** 3833–3841
52. Ishihara, H., Wang, H., Drewes, L. R., and Wollheim, C. B. (1999) *J. Clin. Invest.* **104,** 1621–1629
53. Zhao, C., Wilson, M. C., Schuit, F., Halestrap, A. P., and Rutter, G. A. (2001) *Diabetes* **50,** 361–366
54. Brun, T., Roche, E., Assimacopoulos-Jeannet, F., Corkey, B. E., Kim, K. H., and Prentki, M. (1996) *Diabetes* **45,** 190–198
55. Schuit, F., De Vos, A., Farfari, S., Moens, K., Pipeleers, D., Brun, T., and

Prentki, M. (1997) *J. Biol. Chem.* **272,** 18572–18579
56. Wang, H., and Iynedjian, P. B. (1997) *Proc. Natl. Acad. Sci. U. S. A.* **94,** 4372–4377
57. Becker, T. C., Noel, R. J, Johnson, J. H., Lynch, R. M., Hirose, H., Tokuyama, Y., Bell, G. I., and Newgard, C. B. (1996) *J. Biol. Chem.* **271,** 390–394
58. Walker, J. E. (1992) *Curr. Opin. Struct. Biol.* **2,** 519–526
59. Stein, D. T., Stevenson, B. E., Chester, M. W., Basit, M., Daniels, M. B., Turley, S. D., and McGarry, J. D. (1997) *J. Clin. Invest.* **100,** 398–403
60. Schuit, F. C., Huypens, P., Heimberg, H., and Pipeleers, D. G. (2001) *Diabetes* **50,** 1–11
61. Virji, M. A., Steffes, M. W., and Estensen, R. D. (1978) *Endocrinology* **102,** 706–711
62. Kunz, W. S., and Davis, E. J. (1991) *Arch. Biochem. Biophys.* **284,** 40–46
63. Skulachev, V. P. (1998) *Biochim. Biophys. Acta.* **1363,** 100–124
64. Chan, C. B., De Leo, D., Joseph, J. W., McQuaid, T. S., Ha, X. F., Xu, F., Tsushima, R. G., Pennefather, P. S., Salapatek, A. M., and Wheeler, M. B. (2001) *Diabetes* **50,** 1302–1310
65. Chan, C. B., MacDonald, P. E., Saleh, M. C., Johns, D. C., Marban, E., and Wheeler, M. B. (1999) *Diabetes* **48,** 1482–1486
66. Lameloise, N., Muzzin, P., Prentki, M., and Assimacopoulos-Jeannet, F. (2001) *Diabetes* **50,** 803–809
67. Zhang, C. Y., Baffy, G., Perret, P., Krauss, S., Peroni, O., Grujic, D., Hagen, T., Vidal-Puig, A. J., Boss, O., Kim, Y. B., Zheng, X. X., Wheeler, M. B., Shulman, G. I., Chan, C. B., and Lowell, B. B. (2001) *Cell* **105,** 745–755
68. Weir, G. C., Laybutt, D. R., Kaneto, H., Bonner-Weir, S., and Sharma, A. (2001) *Diabetes* **50,** S154–S159